Geochemistry Geophysics Geosystems G3
AN ELECTRONIC JOURNAL OF THE EARTH SCIENCES
Published by AGU and the Geochemical Society

Article
Volume 9, Number 3
26 March 2008
Q03023, doi:10.1029/2007GC001771
ISSN: 1525-2027

Deepwater circulation on Blake Outer Ridge (western North Atlantic) during the Holocene, Younger Dryas, and Last Glacial Maximum

Helena K. Evans and Ian R. Hall

School of Earth, Ocean and Planetary Science, Cardiff University, Main Building, Park Place, Cardiff CF10 3YE, UK (hall@cardiff.ac.uk)

[1] Three depth transects containing a total of 33 sediment cores were investigated along the Blake Outer Ridge in the western subtropical North Atlantic. Sortable silt mean ($\overline{SS}$) grain size and stable isotope records were used to assess the position and relative intensity of the Western Boundary Undercurrent (WBUC) during the Holocene, the Last Glacial Maximum (LGM), and the Younger Dryas (YD) intervals. The Holocene reconstruction is consistent with modern physical and chemical hydrographic measurements in the area, suggesting a deep position for the fast flowing core of the WBUC (3000–4000 m, deepening to ~4500 m water depth on the ridge flanks) and a water column dominated by North Atlantic Deep Water (NADW). The LGM and YD reconstructions show that a comparable hydrographic regime was present during both these intervals, suggesting a similar mode of circulation that was appreciably different from the Holocene reconstruction. The WBUC's zone of maximum flow speed during these intervals is suggested to have shifted above 2500 m water depth, consistent with nutrient depleted Glacial North Atlantic Intermediate Water formation with an increasing influence of Southern Source Water (SSW) beneath. Below 4000 m water depth, $\overline{SS}$ results hint at increased SSW flow vigor during both the LGM and YD with higher flow speeds than during the Holocene. This study provides a framework for aiding the interpretation of time series records of paleocurrent flow speed changes in the region of the WBUC.

Components: 12,206 words, 6 figures, 2 tables.

Keywords: Western Boundary Undercurrent; sortable silt; Holocene; Last Glacial Maximum; Younger Dryas.

Index Terms: 4999 Paleoceanography: General or miscellaneous; 4962 Paleoceanography: Thermohaline; 4924 Paleoceanography: Geochemical tracers.

Received 29 July 2007; **Revised** 20 December 2007; **Accepted** 26 December 2007; **Published** 26 March 2008.

Evans, H. K., and I. R. Hall (2008), Deepwater circulation on Blake Outer Ridge (western North Atlantic) during the Holocene, Younger Dryas, and Last Glacial Maximum, *Geochem. Geophys. Geosyst.*, *9*, Q03023, doi:10.1029/2007GC001771.

1. Introduction

[2] The deep western boundary current (DWBC) on the western Atlantic margin (regionally known as the Western Boundary Undercurrent, WBUC) transports recently ventilated North Atlantic Deep Water (NADW) along the Northeast American continental margin toward the Blake Outer Ridge (BOR), a 700 km long sediment drift in the subtropical Atlantic Ocean (Figure 1). For the most part, NADW flow is strongly constrained by bottom topography, with the most recently ventilated

Copyright 2008 by the American Geophysical Union

waters located adjacent to the steepest parts of the continental margin [*Johns et al.*, 1997]. Deep Western Boundary Current volume transports of between 16–19 Sv have been recorded for water flowing equatorward below a potential temperature of 6°C at the BOR [*Stahr and Sanford*, 1999], of which 7.6 Sv is lower (L)NADW [*Orsi et al.*, 2001]. Current speeds of 10–30 cm s^{-1} have been both measured and estimated from geostrophic calculations [e.g., *Amos et al.*, 1971; *Hogg*, 1983; *Stahr and Sanford*, 1999]. It has been suggested from both observations [e.g., *Mix and Fairbanks*, 1985; *Lea and Boyle*, 1990; *Haskell et al.*, 1991; *Alley et al.*, 1993] and numerical models [e.g., *Manabe and Stouffer*, 1997] that changes in the WBUC are indicative of changes in the climate as this current is an important component of the global thermohaline circulation system.

[3] Grain size analysis potentially provides a direct measure of near bottom flow speeds and in regions of drift deposits such as the BOR, gives insights into deepwater circulation patterns, intensity and complements information gained from geochemical tracers related to hydrography. Here we present results of an investigation aimed at the comparison of sedimentological parameters in relation to deepwater circulation patterns on the BOR for both the Holocene and during past climate extremes, e.g., the Last Glacial Maximum (LGM) and Younger Dryas (YD). In order to achieve this we employ the mean grain size of the terrigenous 10–63 μm fraction, hereafter termed sortable silt mean ($\overline{SS}$), which is suggested to be primarily current sorted [*McCave et al.*, 1995; *McCave and Hall*, 2006], with high values representing stronger relative near-bottom current speeds and vice versa. The $\overline{SS}$ proxy can be used where the source sediment is characterized by a broad range of grain sizes and the distance to the core site is sufficient for a sorted signal to develop [*McCave et al.*, 1995; *Bianchi et al.*, 2001; *McCave and Hall*, 2006]. These conditions are met on the BOR where terrigenous sediment supply is principally via material being transported by the WBUC [*Heezen et al.*, 1966] from the American continental margin.

[4] We first aim to reconstruct average Holocene physical and chemical hydrography at the BOR in order to ground truth the $\overline{SS}$ proxy against modern physical hydrographic studies such as that of *Stahr and Sanford* [1999], which describes in detail the present flow regime of the WBUC at the BOR (Figure 2). Similar studies have been undertaken previously by *Haskell and Johnson* [1993] on BOR and upstream on the continental margin at ~36–42°N from 3000 m to 4900 m water depth by *Ledbetter and Balsam* [1985]. However, our study should improve upon these findings as we employ the $\overline{SS}$ proxy, which provides a more sensitive indicator of near bottom current flow than the "total" detrital silt fraction (6–70 μm [*Haskell and Johnson*, 1993]; 4–63 μm [*Ledbetter and Balsam*, 1985]) size ranges. Furthermore, we compare stable carbon isotopes measured on benthic foraminifera from the Holocene with previously published core top benthic $\delta^{13}C$ from the BOR [*Keigwin*, 2004] and $\delta^{13}C$ transects through the western Atlantic [*Curry and Oppo*, 2005] in order to firmly establish the chemical hydrography of the region. Extending the same proxy suite we aim to reconstruct the hydrographic setting during the LGM and YD (where the age control is sufficiently well constrained) when, climatically conditions should have been most different from the Holocene. A comparison of these three time intervals will enable examination of the spatial extent of any vertical shifts in the zone of maximum flow speeds within the WBUC and hydrographic changes between Northern and Southern Source Water (NSW/SSW).

1.1. Regional Setting

[5] The BOR slopes to the southeast between ~2000 and 5000 m water depth and is believed to have formed through interaction between the upper part of the WBUC and the lower part of the Gulf Stream (Florida Current) where it detaches from the continental slope [*Bryan*, 1970; *Stahr and Sanford*, 1999]. These currents erode and transport sediments originating from the continental margin to the north and Blake Plateau to the south toward the BOR [*Ewing et al.*, 1966; *Heezen et al.*, 1966; *Laine et al.*, 1994].

[6] Current-controlled sediment deposition at the BOR is influenced by each of the climatically important water masses of the WBUC [*Stahr and Sanford*, 1999]. The depth boundaries of these water masses overlie each other, reflecting both a deepening of the WBUC flow along the ridge crest and the fact that these categories are partly based on an amalgamation of prior definitions [*Stahr and Sanford*, 1999]. The uppermost water mass is a shallow component of Labrador Seawater ((S)LSW, 1000–1800 m water depth) and this is underlain by LSW (1400–2800 m water depth). These water masses from the Labrador Sea collectively form Upper (U)NADW, with LNADW (2500–4100 m

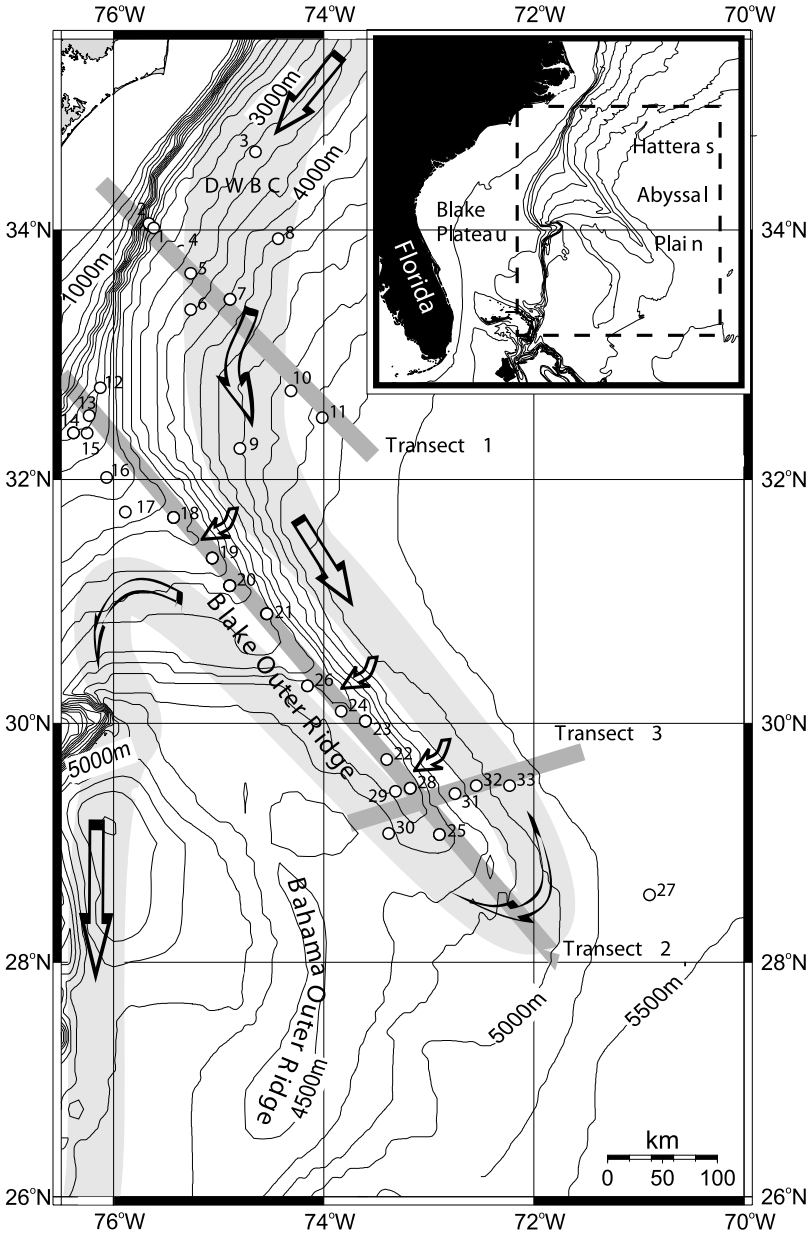

Figure 1. Bathymetric map of the study area showing the locations of the three transects used in this study. The core sites are numbered following the Map ID column in Table 1. The large arrows and the shaded area represent the fast flowing core of the DWBC [after *Johns et al.*, 1997; *Stahr and Sanford*, 1999].

water depth) and deep Bottom Water (BW, >3400 m water depth to the bottom) below. This latter water mass consists of a varying mixture of NSW (84–90%) and SSW (10–16%) [*Stahr and Sanford*, 1999], where the southern component has been recirculated in a cyclonic gyre north of the BOR [*Amos et al.*, 1971; *Stahr and Sanford*, 1999], and therefore has the same flow direction as the overlying LNADW at the BOR [*Weatherly and Kelley*, 1984]. North of BOR the maximum flow speeds in the WBUC are found in this water mass and its boundary with overlying LNADW [*Richardson et al.*, 1981; *Weatherly and Kelley*, 1984; *Bulfinch et al.*, 1982; *Bulfinch and Ledbetter*, 1983–1984].

[7] The present-day fast flowing primary core of the WBUC, with velocities >15 cm s^{-1} at the BOR, is located between 3500 m water depth near the upstream origin (influencing depths as shallow as 3000 m) and 4100 m further downstream along the eastern flank [*Stahr and Sanford*, 1999]. The

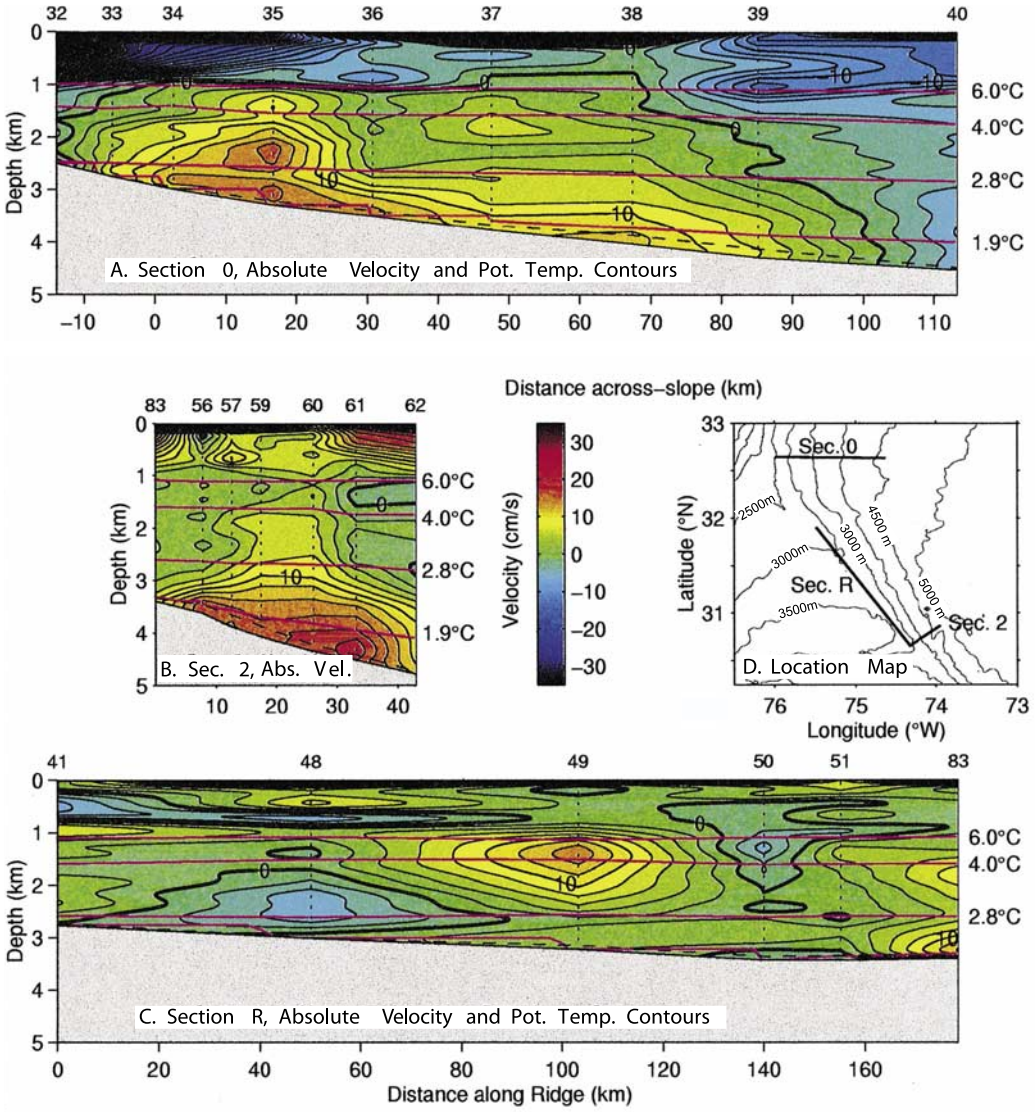

Figure 2. Contours of absolute velocity component normal to the sections and potential temperature at the Blake Outer Ridge, July 1992. Contour intervals are every 5 cm s^{-1}. The coordinate system is along-stream with positive flow equatorward. Potential temperature contours that divide transport categories are labeled to the right of each contour plot. The height of the bottom mixed layer is indicated by the dashed line near the bottom. Figure 2a is Section 0, Figure 2b is Section 2, and Figure 2c is Section R. Figure 2d is a map to clarify section locations (from *Stahr and Sanford* [1999], with permission from Elsevier.

position and strength of this fast flowing WBUC core have been shown to vary in both space (depth) and time [*Ledbetter and Balsam*, 1985; *Bianchi et al.*, 2001; *Yokokawa and Franz*, 2002] in response to changes in source water production and intensity [*Pickart*, 1992]. *Johns et al.* [1997] and *Stahr and Sanford* [1999] also document a secondary fast flowing core within (S)LSW (~1000–2500 m water depth) which is less constrained by topography than the deeper core.

1.2. Past Paleocurrent Reconstructions From the BOR

[8] Several investigations have utilized sedimentary grain size measurements at the BOR with the intention of reconstructing the strength and flow characteristics of the WBUC on millennial to Milankovitch timescales. Early grain size studies attempted to reconstruct the paleocurrent intensity of the WBUC along the crest of the BOR [*Johnson et al.*, 1988], where variations in grain size at one

location on the ridge crest could be a response to both fluctuations in the strength of the WBUC and changes in the depth of the fast flowing core [*Ledbetter and Balsam*, 1985; *Johnson et al.*, 1988]. *Haskell et al.* [1991] investigated four sites spanning 2650–3818 m water depth and concentrated on determining changes in the WBUC flow characteristics since the LGM. *Haskell et al.* [1991] suggested that prior to 12 ka B.P. circulation was focused on the upper part of the ridge above 2700 m water depth, which may have corresponded to increased production of intermediate waters in the North Atlantic at this time. Furthermore, opposing trends in the shallow and deep cores suggest that two independent circulation patterns were in operation at the top and bottom of the ridge during the deglacial period. The first attempt at reconciling the modern hydrography at the BOR with grain size measurements from core top samples was made by *Haskell and Johnson* [1993]. This study, using the mean size of the detrital silt and very fine sand fraction (6–70 μm), suggested that modern sediment texture and composition on the flanks of the BOR was influenced by the WBUC, but proximity to the continental slope and distance from the upstream sediment source areas dominated the grain size signal down the crest of the ridge. There was no direct indication of WBUC influence recorded in the sediment properties on the crest of the ridge, even where the WBUC fast flowing core crosses the ridge above 4200 m water depth.

[9] Several recent paleocurrent studies followed Ocean Drilling Program (ODP) Leg 172. *Bianchi et al.* [2001] used ODP Sites 1060 (3481 m water depth) and 1062 (4763 m water depth) to reconstruct the physical and hydrographic conditions during marine isotope stages (MIS) 6-5d (~130–110 ka B.P.). A combination of the $\overline{SS}$ and benthic $\delta^{13}C$ were used to reconstruct the intensity and position of the fast flowing core of the WBUC during MIS 5e (~4000 m) and suggested that changes in the LNADW/SSW ratio were accompanied by vertical shifts in the WBUC's zone of maximum flow speed, which appeared to shoal in response to a reduced presence of LNADW. *Yokokawa and Franz* [2002] focused on the time interval from 350–250 ka B.P. (MIS 10.2–8.3) at ODP Sites 1055–1062 (1800 m to 4760 m water depths), using a combination of grain size measurements and magnetic properties (anisotropy of the magnetic susceptibility). They suggest that the zone of maximum speed in the WBUC was located at ~2200 m water depth during the glacial periods (MIS 10.2 and 8.4–8.3), deepening to >3000 m water depth during the warm intervals (MIS 9.3 and 8.5). Sedimentological properties have also been combined with stable isotope data during the MIS 12–10 interval at Site 1061 (4047 m water depth [*Hall and Becker*, 2007]. These results suggest MIS 12 was associated with a shallower zone of maximum flow speed within the WBUC, consistent with decreased LNADW influence and a high contribution of southern origin water at depth. During peak interglacial conditions (MIS 11.3) there was evidence for a deep flowing high velocity core within the WBUC and stronger LNADW influence. Finally, in a detailed study of MIS 3 at ODP Site 1060, *Hoogakker et al.* [2007] suggest that many perturbations of the WBUC flow are related to SSW variability and were correlated with temperature and inferred hydrographic changes around Antarctica.

2. Materials and Methods

[10] Thirty three sediment cores were sampled along three transects at the BOR in order to study how circulation patterns on different parts of the ridge affect surface sediment properties (Figure 1 and Table 1). The cores were collated from several different research cruises. Cores recovered during R/V *Knorr* (KNR) and R/V *Atlantis* II (AII) cruises were sampled at the repository at Woods Hole Oceanographic Institution (WHOI), while those cores from the R/V *Vema* (VM) and R/V *Robert Conrad* (RC) cruises were sampled at Lamont-Doherty Earth Observatory (L-DEO), at Columbia University, USA. The first transect (hereafter T1) was positioned across the slope and rise upstream of the ridge with the purpose of capturing the entire width of the WBUC as it enters the region of the BOR. This transect is located close to "Section 0" of *Stahr and Sanford* [1999] (Figure 2a). The second location (hereafter T2) forms a depth transect running along the crest of the ridge, similar to the ridge crest transect of *Haskell and Johnson* [1993] and hydrographic "Section R" of *Stahr and Sanford* [1999] (Figure 2c). Previous studies utilizing sediment cores from the crest of the BOR [e.g., *Haskell and Johnson*, 1993; *Bianchi et al.*, 2001; *Keigwin and Schlegel*, 2002; *Keigwin*, 2004] have highlighted the presence of high sedimentation rates (up to ~60 cm ka^{-1}) providing an opportunity to obtain millennial-scale, or better, resolution records suggesting the potential for further paleoceanographic work. Transect 3 (hereafter T3) is a small transect traversing the northeast side of the BOR and is at a similar location to the

Table 1. Locations, Water Depths, and Sampling Intervals for Blake Outer Ridge Cores[a]

Store	Core ID	Lat.	Long.	Depth, m	Holo, cm	Glacial (LGM), cm	YD, cm	Stratigraphy	Ref	Map ID
					Transect 1					
WHOI	AII72-21PC	34.1	−75.7	2202	0–15	120–160	-	MS/δ^{18}O	a	1
WHOI	AII72-22PC	34.0	−75.6	2942	0–15	70–100	-	MS/δ^{18}O	a	2
LDEO	VM30-5	34.6	−74.7	3203	0–25	-	-	MS/δ^{18}O	a	3
WHOI	AII72-23PC	33.8	−75.3	3204	0–25	60–90	-	MS/δ^{18}O	a	4
LDEO	RC9-4	33.4	−75.3	3552	0–15	130–170	-	MS/δ^{18}O	a	5
WHOI	AII72-24PC	33.4	−74.9	3824	0–15	70–120	-	MS/δ^{18}O	a	6
LDEO	VM26-175	33.9	−74.4	3995	0–25	120–170	-	MS/δ^{18}O	a	7
LDEO	RC7-2	32.3	−74.8	4398	0–10	240–260	-	MS/δ^{18}O	a	8
LDEO	VM30-7	32.7	−74.4	4702	0–10	-	-	MS/δ^{18}O	a	9
LDEO	RC1-10	32.5	−74.0	4892	0–10	110–130	-	MS/δ^{18}O	a	10
WHOI	AII72-16PC	32.5	−73.5	5058	-	120–160	-	MS/δ^{18}O	a	11
					Transect 2					
WHOI	KNR140/2-50GGC	32.7	−76.2	2155	0–170	240–280	180–200	δ^{18}O/BFA	b	12
WHOI	KNR140/2-66GGC	32.5	−76.3	2155	0–50	120–160	77–87	δ^{18}O/BFA	b	13
WHOI	KNR140/2-1JPC	32.3	−76.4	2243	0–73	130–165	91–96	δ^{18}O/BFA	b	14
WHOI	KNR140/2-46GGC	32.3	−76.3	2320	0–78	218–238	-	δ^{18}OBFA	b	15
WHOI	KNR140/2-43GGC	32.0	−76.1	2590	0–35	167–215	59–67	δ^{18}OBFA	b	16
WHOI	KNR140/2-42GGC	31.7	−75.9	2710	0–10	130–170	-	MS/δ^{18}O	a	17
WHOI	KNR140/2-39GGC	31.7	−75.4	2975	0–100	300–450	125–130	Δ14C/δ^{18}O	c	18
WHOI	KNR140/2-36JPC	31.4	−75.1	3007	0–15	200–300	-	MS/δ^{18}O	a	19
WHOI	KNR140/2-33JPC	31.1	−74.9	3315	-	200–300	-	MS/δ^{18}O	a	20
WHOI	KNR140/2-31GGC	30.9	−74.5	3410	0–50	300–400	105–125	δ^{18}O/BFA	b	21
WHOI	KNR140/2-26GGC	29.7	−73.4	3845	0–40	320–400	-	δ^{18}O/BFA	b	22
WHOI	KNR140/2-29GGC	30.0	−73.6	3978	0–30	400–450	39–63	δ^{18}O/BFA	b	23
WHOI	KNR140/2-28GGC	30.1	−73.8	4211	0–24	260–360	53–60	δ^{18}O/BFA	b	24
WHOI	KNR140/2-12JPC	29.1	−72.9	4250	-	268–378	73–85	δ^{18}O/BFA	b	25
LDEO	RC16-7	30.3	−74.1	4893	-	50–70	-	MS/δ^{18}O	a	26
LDEO	VM25-2	28.6	−71.1	5409	0–10	50–75	-	MS/δ^{18}O	a	27
					Transect 3					
WHOI	KNR140/2-25PC	29.6	−73.2	3865	0–10	25–40	-	MS/δ^{18}O	a	28
LDEO	RC9-10	29.4	−73.3	4277	0–10	30–60	-	MS/δ^{18}O	a	29
LDEO	VM22-6	29.1	−73.3	4499	0–15	50–80	-	MS/δ^{18}O	a	30
LDEO	RC9-13	29.4	−72.7	4735	0–10	80–90	-	MS/δ^{18}O	a	31
LDEO	RC9-12	29.5	−72.5	4958	0–10	40–70	-	MS/δ^{18}O	a	32
LDEO	RC9-11	29.5	−72.2	5212	-	20–40	-	MS/δ^{18}O	a	33

[a] The stratigraphy column gives an indication of the methods used to locate the time interval of interest, where MS is magnetic susceptibility measurements, δ^{18}O is planktonic oxygen isotope stratigraphy, BFA is benthic foraminifera abundance peaks, and Δ^{14}C is existing AMS radiocarbon dates. Reference a, this study; b, *Keigwin* [2004]; c, *Keigwin and Schlegel* [2002]. The location of the cores can be found on Figure 1 using the MAP ID in the final column.

across-ridge transect of *Haskell and Johnson* [1993] and hydrographic "Section 2" of *Stahr and Sanford* [1999] (Figure 2b). The northeast side of the BOR was chosen as previous studies have shown the presence of a strong current with no indication of a recirculation gyre [*Haskell and Johnson*, 1993; *Johns et al.*, 1997], which can prove difficult to separate from the equatorward flow of the WBUC where both are present [*McCartney*, 1993]. The nearest reported gyre is to the south in the Blake Abyssal Basin at 26.5°N [*Lee et al.*, 1996; *Johns et al.*, 1997; *Leaman and Vertes*, 1996].

[11] On average 3–5 sub-samples were taken, where possible, from each core during the Holocene, LGM and YD time intervals in order to obtain an average grain size measurement covering a range of water depths for each time period under investigation. All of the sediment sub-samples collected were wet sieved through 63 μm sieves and both the "fine" and "coarse" fractions were preserved, dried and weighed following the sample preparation procedures described by *Bianchi et al.* [2001]. All $\overline{SS}$ grain size measurements were initially carried out on the Coulter Counter Multisizer III, following the methods described by *Bianchi et al.* [2001]. Measurements were made

Table 2. Radiocarbon ^{14}C AMS Dating Results From Cores KNR 140/2-66GGC, KNR 140/2-43GGC, and KNR 140/2-28GGC With a Marine Reservoir Correction of −400 Years[a]

Laboratory Number	Material	Depth, cm	^{14}C Age, years B.P.	Error Age ±1σ, years B.P.	Calendar Age, years
			66GGC		
SUERC-7716	*G. ruber*	49–50	6737	24	7595
SUERC-7717	*G. ruber*	77–78	10427	40	11548
SUERC-7720	*G. ruber*	93–94	12591	40	14046
SUERC-7722	*G. ruber*	111–112	12067	38	13505
SUERC-7723	*G. ruber*	129–130	15990	60	18864
SUERC-7724	*G. ruber*	162–163	21243	114	25122
			43GGC		
SUERC-7710	*G. ruber*	35–36	7347	25	7814
SUERC-7712	*G. ruber*	67–68	11727	36	13207
SUERC-7713	*G. ruber*	79–80	13172	42	15071
SUERC-7714	*G. ruber*	127–128	15368	55	18389
SUERC-7715	*G. ruber*	167–168	17723	74	20431
			28GGC		
SUERC-7701	*G. ruber*	24–25	9405	29	10324
SUERC-7702	*G. ruber*	48–49	10924	33	12439
SUERC-7703	mixed	89–90	12891	41	14596
SUERC-7704	mixed	152–157	13613	45	15633
SUERC-7705	mixed	207.5–209	14303	48	16558
SUERC-7707	mixed	261–263	14664	51	17037

[a] Obtained from CALIB v5.0.1 program [*Stuiver et al.*, 2005].

on the <63 μm terrigeneous fraction following the removal of the biogenic carbonate and silica by slow acid digestion in 1M acetic acid solution followed by heating in a 2M solution of sodium carbonate (Na_2CO_3) in a water bath at 85°C for 5 hours. Additional grain size measurements were undertaken using the Sedigraph 5100 in order to determine the sortable silt abundance (SS%) and silt/clay ratio. The SS% was found to vary in the range of 5–15% enabling the determination of the $\overline{SS}$ with an analytical error of 2–3% [*Bianchi et al.*, 1999].

[12] Stable isotope ($\delta^{18}O$ and $\delta^{13}C$) analyses were carried out on both planktonic and benthic foraminifera in order to reconstruct water mass properties and provide additional chronological support (see below). For planktonic isotopic measurements ~30 specimens of the species *Globigerinoides ruber* (white) were picked from the 150–250 μm fraction. Additionally when abundant benthic foraminifera were available, 2–3 specimens of *Cibicidoides spp.* were selected from the >150 μm fraction for analysis. All analyses were performed using a Finnigan MAT252 mass spectrometer with automated Kiel carbonate preparation device at Cardiff University. External reproducibility was monitored through repeat measurements of an internal laboratory standard and was 0.03‰ for $\delta^{13}C$ and 0.08‰ for $\delta^{18}O$. All isotope values are related to the Vienna Peedee Belemnite scale (VPDB) through repeated analyses of National Bureau of Standards isotopic standard reference material NBS-19. Benthic $\delta^{18}O$ values have been shifted by +0.64‰ to accommodate offset of *Cibicidoides spp.* from oxygen isotope equilibrium [*Shackleton*, 1974]. In contrast to the $\overline{SS}$ record which is continuous, since terrigenous silts are ubiquitous, the benthic foraminiferal stable isotope records are patchy as suitable benthic foraminifera are not found in all samples due to the small sample size available for analyses, dissolution of the calcareous shells (particularly at the deeper sites below ~3000 m water depth) and dilution due to high sedimentation rates (particularly along the ridge crest).

3. Chronology

[13] Several techniques were used to develop preliminary chronologies for each of the core sites. New ^{14}C AMS dates are presented for three cores: KNR 140/2-66GGC, KNR 140/2-43GGC and KNR 140/2-28GGC (Table 2), while the age model of *Keigwin and Schlegel* [2002] is used to provide the stratigraphic control for core KNR 140/2-39GGC. Previously published planktonic isotope

stratigraphies and individual ^{14}C AMS dates [*Keigwin*, 2004] were used to constrain the Holocene (last 10 ka B.P.), LGM (interval centered on 21 ka B.P. with a duration of a few millennia [*Lynch-Steiglitz et al.*, 2007]) and YD (13–11.5 ka B.P.) in the remaining KNR cores. Additionally, benthic foraminifera abundance peaks have been previously observed in many instances (but not exclusively) to correspond with maxima in the planktonic $\delta^{18}O$ record consistent with YD cooling and to a lesser extent the LGM at the BOR [*Keigwin and Schlegel*, 2002; *Keigwin*, 2004] (see auxiliary material[1] Figure S1) providing a further stratigraphic marker. The cause of these benthic foraminifera abundance peaks is unclear although *Keigwin* [2004] speculated that temporal changes in surface ocean productivity documented elsewhere in the ocean may be related [e.g., *Zahn et al.*, 1986; *Loubere*, 1991, 2000; *Keigwin et al.*, 1992].

[14] For the remaining core sites, without existing isotope stratigraphies, accurate age determinations were more difficult and only the Holocene and LGM were sampled, as locating the YD proved too speculative. A combination of magnetic susceptibility and color variations of the sediment were used to locate the Holocene and the LGM in the remaining cores (see auxiliary material Figure S2). Sediments from the LGM are generally clay-rich and show higher magnetic susceptibility, whereas carbonate-rich sediments dominate in the interglacial periods and show low magnetic susceptibility. Sediments deposited at the BOR at the time of the LGM are condensed and contain red silt and clay from the Carboniferous and Triassic of the Canadian Maritime Provinces, delivered into the WBUC by turbidity currents at glacial low sea level [*Heezen et al.*, 1966; *Hollister and Heezen*, 1972; *Barranco et al.*, 1989]. This contrasts with finer, green-brown overlying Holocene sediments. The color transition between glacial and interglacial periods is typical of other cores in the region [*Keigwin et al.*, 1998] and can be used to distinguish between cold and warm periods.

[15] Benthic foraminifera are too sparse to provide detailed benthic $\delta^{18}O$ time series throughout each core, hindering the identification of the various study intervals from the glacioeustatic signal. However, a depth transect of benthic $\delta^{18}O$ values for the Holocene, LGM and YD has been achieved (Figure 6a), with values for the Holocene (~2.7‰) and LGM (~4.25‰) consistent with those previously published by *Keigwin* [2004] from the BOR and *Curry and Oppo* [2005] from a transect through the western North Atlantic. Unsurprisingly the YD benthic $\delta^{18}O$ values lie between the Holocene and LGM values at ~3.4‰. There is also consistency between samples from individual time periods allowing further confidence that comparable intervals have been sampled and analyzed. Finally, the planktonic $\delta^{18}O$ of *G. ruber* (white) were analyzed for each sub-sample (Figure 3) in order to check that the samples selected were consistent with regional planktonic $\delta^{18}O$ values for the three time-slices chosen for investigation. The planktonic $\delta^{18}O$ results were also collected to study isotopic changes with depth of sample recovery and distance away from the continental margin.

4. Results

4.1. Surface Reconstructions

[16] The mean Holocene planktonic $\delta^{18}O$ values increase gradually by ~0.5‰ with water depth along the BOR from around −1.3‰ to −0.8‰ (Figure 3). The range of this increase is consistent with the previous planktonic $\delta^{18}O$ depth transects at the BOR [e.g., *Keigwin*, 2004]. The absolute values however are slightly heavier than in the study of *Keigwin* [2004], which is likely to result from *Keigwin* [2004] measuring core top samples while this study estimates an average Holocene $\delta^{18}O$ value. Our mean Holocene $\delta^{18}O$ values at the shallow sites close to the continental margin on the BOR are ~1‰ lower than the previously published Bermuda Rise data [*Keigwin*, 1996; *McManus et al.*, 2004], which is consistent with the 4°C temperature difference between these locations today [*Keigwin*, 2004]. The mean LGM planktonic $\delta^{18}O$ values also increase seaward similar to the Holocene data, but values are typically ~1.8‰ heavier than during the Holocene. This is comparable to the ~2‰ difference between these time periods suggested by *Keigwin* [2004]. The mean YD planktonic $\delta^{18}O$ values are intermediate between the Holocene and LGM data, suggesting that the sea surface temperatures were warmer in the subtropical North Atlantic at this time compared with the LGM but cooler than the Holocene.

4.2. Deep Hydrography

4.2.1. Grain Size

[17] All transects during the three time intervals reveal a changing pattern of $\overline{SS}$ with depth

[1] Auxiliary materials are available in the HTML. doi:10.1029/2007GC001771.

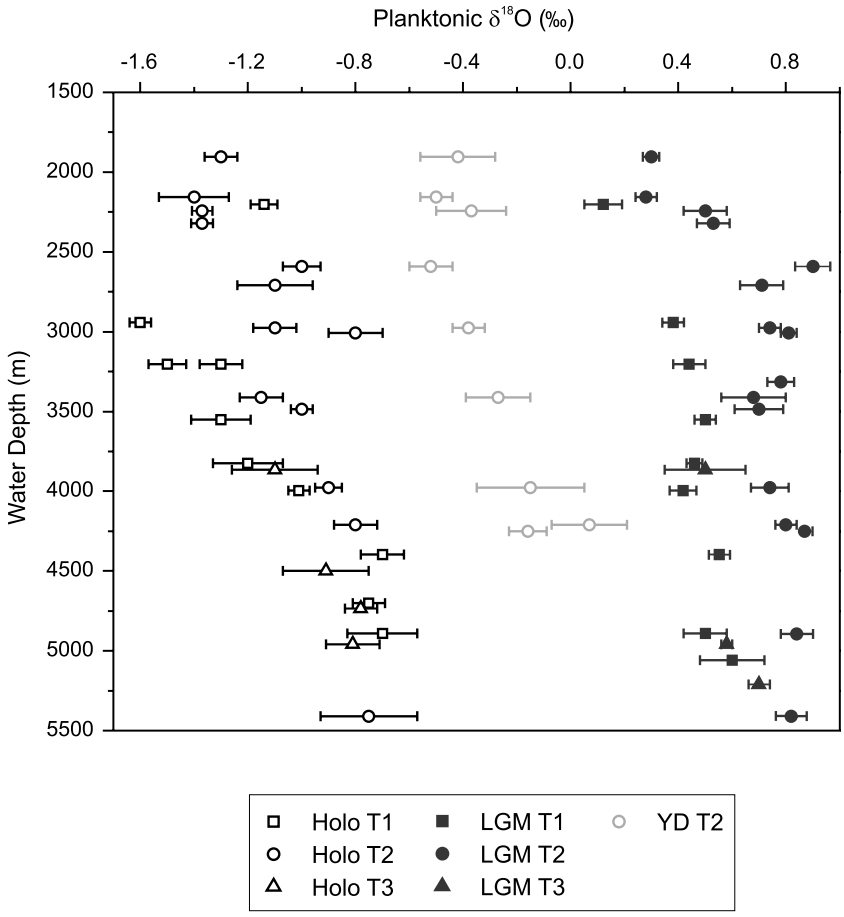

Figure 3. Trends in average planktonic $\delta^{18}O$ from the Holocene (black), LGM (light grey), and YD (dark grey) time slices as a function of water depth. Samples from transect 1 are shown by squares, samples from transect 2 are shown by circles, and samples from transect 3 are shown by triangles. Each point represents an average value of 3–5 measurements with bars showing the 1σ standard deviation at each depth.

(Figure 4). The Holocene reconstruction shows a region of coarse $\overline{SS}$ at both Transects 1 and 2 between ~3000 m and 4000 m water depth, suggesting a region of relative fast flow speeds at this depth, consistent with modern hydrographic reconstructions of the fast flowing core of the WBUC with flow speeds >15 cm s^{-1} [e.g., *Stahr and Sanford*, 1999] (Figures 2, 4a, and 4b). This coarsening in the $\overline{SS}$ dominates the grain size signal at T1. At T2 the Holocene $\overline{SS}$ average over the depth range of the modern zone of maximum WBUC flow, although high, has lower $\overline{SS}$ values than at T1 (~16.5 μm at T2 compared with ~18.5 μm at T1). This is suggestive of a possible slowing of the WBUC between T1 and T2. An increase in $\overline{SS}$ is also apparent at T2 at shallower depths <2300 m, consistent with the location of the modern shallow secondary core of the WBUC which is presently (S)LSW-sourced [*Johns et al.*, 1997]. As there is only a single data point shallower than 2300 m water depth at T1 it is unclear as to whether this transect is also influenced by the shallow secondary core of the WBUC. Below 4000 m water depth, the Holocene $\overline{SS}$ shows a decreasing trend at both T1 and T2 consistent with a decreasing influence of the deep fast flowing core of the WBUC. T1 reaches a minimum value of ~14.3 μm at 4750 m water depth, while T2 reaches a minimum of 15.3 μm at 4211 m water depth. T3 was designed to study the deepest component of the flow regime on the BOR and transect consisting of 6 data points covering a depth range of 3865–5212 m (Figure 4c). However, this is sufficient to resolve the main flow characteristics at depth. Similarly to T1 and T2, the Holocene T3 also suggests coarser $\overline{SS}$ values consistent with the position of the fast flowing core of the WBUC, but with coarse values reaching a greater depth of 4500 m.

[18] The LGM reconstruction indicates that an appreciably different hydrographic setting was

present at this time compared with the Holocene and this is further highlighted by the deviation (Holocene-LGM) graphs in the right side of Figure 4. In all 3 transects the ~3000–4000 m depth range of the Holocene $\overline{SS}$ maximum shows a minimum in grain size for the LGM, with $\overline{SS}$ values 1.5–2.5 μm finer than during the Holocene. The decrease in $\overline{SS}$ is greater than the 1σ variance on the Holocene and LGM samples suggesting that these data are statistically distinct. All three transects suggest that below 4000 m water depth $\overline{SS}$ values increase to higher values than those associated with the Holocene reconstruction, suggesting faster flow speeds below ~4000 m water depth in the LGM compared to the Holocene. The T1 and T2 depth reconstructions further imply that shallower depths (<2500 m) also experienced relatively faster flows during the LGM, with $\overline{SS}$ values reaching 19.4 μm at 2202 m water depth and 20.3 μm at 2155 m water depth, respectively (Figures 4a and 4b), consistent with more vigorous intermediate depth flow speeds during the last glacial than the Holocene.

[19] The YD reconstruction was limited to a selection of core sites on T2 (Figure 4b) with published stratigraphies [*Keigwin*, 2004], and the highest sedimentation rates presenting the largest sampling interval during the YD interval. The $\overline{SS}$ results for the YD reconstruction suggest a very similar grain size pattern to the LGM along the crest of the ridge. The $\overline{SS}$ values peak at ~19.0 μm at 2155 m water depth and reach a minimum of 15.0 μm at 3978 m water depth, which is similar in both magnitude and depth to the LGM reconstruction. Although the YD transect has only two data points deeper than 4000 m water depth, these hint at increasing grain size values below this depth, higher than Holocene values, consistent with the LGM reconstruction.

[20] The Holocene silt/clay ratios along T2 on the crest of the BOR, show a weak negative correlation with water depth (R^2 = 0.36 (excluding the data point at 5,409 m water depth); Figure 5). Values decrease from ~1.1 at ~2,250 m water depth to ~0.4 at ~4,250 m water depth. These data highlight the previously reported general trend of increasing clay and decreasing silt abundances with water depth, suggesting that the mean grain size of the "total" silt fraction recorded by *Haskell and Johnson* [1993] was significantly influenced by the cohesive grains <10 μm.

4.2.2. Benthic δ^{13}C and δ^{18}O

[21] The benthic δ^{18}O and δ^{13}C results are shown in Figures 6a and 6b and provide additional Holocene and LGM profiles at the BOR to the previous time slice reconstructions published by *Keigwin* [2004], with the addition of a low resolution YD profile. Due to the small number of samples available for analysis, the data from all three transects are plotted together for individual time slices to achieve the largest depth range possible in order to highlight changes in the hydrography of the major water masses. Only the benthic foraminifera *Cibicidoides spp*. have been utilized due to the uncertainties associated with applying a correction factor for the vital effects of *U. peregrina* [*Zahn et al.*, 1986], the second most abundant benthic foraminifera at the BOR.

[22] All three transects show consistent trends when reconstructing the Holocene pattern of benthic δ^{13}C and δ^{18}O in the region of the BOR. The benthic δ^{18}O is used primarily in this study as a stratigraphic marker. The Holocene benthic δ^{13}C reconstruction suggests that waters above ~4000 m are nutrient depleted with values ~1‰, consistent with NADW (Figure 6b). Below ~4000 m water depth the benthic δ^{13}C values decrease to ~0.5‰ suggesting that there is some mixing occurring with poorly ventilated SSW from below. This is consistent with the presence of BW (>3400 m water depth to the bottom [*Stahr and Sanford*, 1999]) which contains a significant component (~10–16%) of SSW (specifically Antarctic Bottom Water [*Amos et al.*, 1971]).

[23] The LGM reconstruction shows a different pattern of benthic δ^{13}C variability with depth (Figure 6b). The LGM is dominated by a decreasing trend in the benthic δ^{13}C with depth, suggesting a shoaling of nutrient-depleted NSW and increasing penetration of nutrient-enriched SSW below. At intermediate water depths (<2500 m), the LGM experiences benthic δ^{13}C values 0.1–0.2‰ greater than during the Holocene, suggesting similar, if not better, ventilation at intermediate depths than during the Holocene, consistent with shoaled NSW [*Came et al.*, 2003; *Marchitto et al.*, 1998; *Keigwin*, 2004; *Curry and Oppo*, 2005]. *Keigwin* [2004] suggests this is a minimum difference between the Holocene and LGM δ^{13}C values because of deglacial secular changes in the δ^{13}C of ΣCO_2 of ~0.3‰ [*Duplessy et al.*, 1988; *Keigwin*, 2004]. The decreasing benthic δ^{13}C values below 2500 m water depth are consistent with an increased influence of nutrient enriched SSW.

[24] Only a few benthic δ^{13}C values are available for the YD (Figure 6b), which may seem surprising given the occurrence of benthic foraminifera abun-

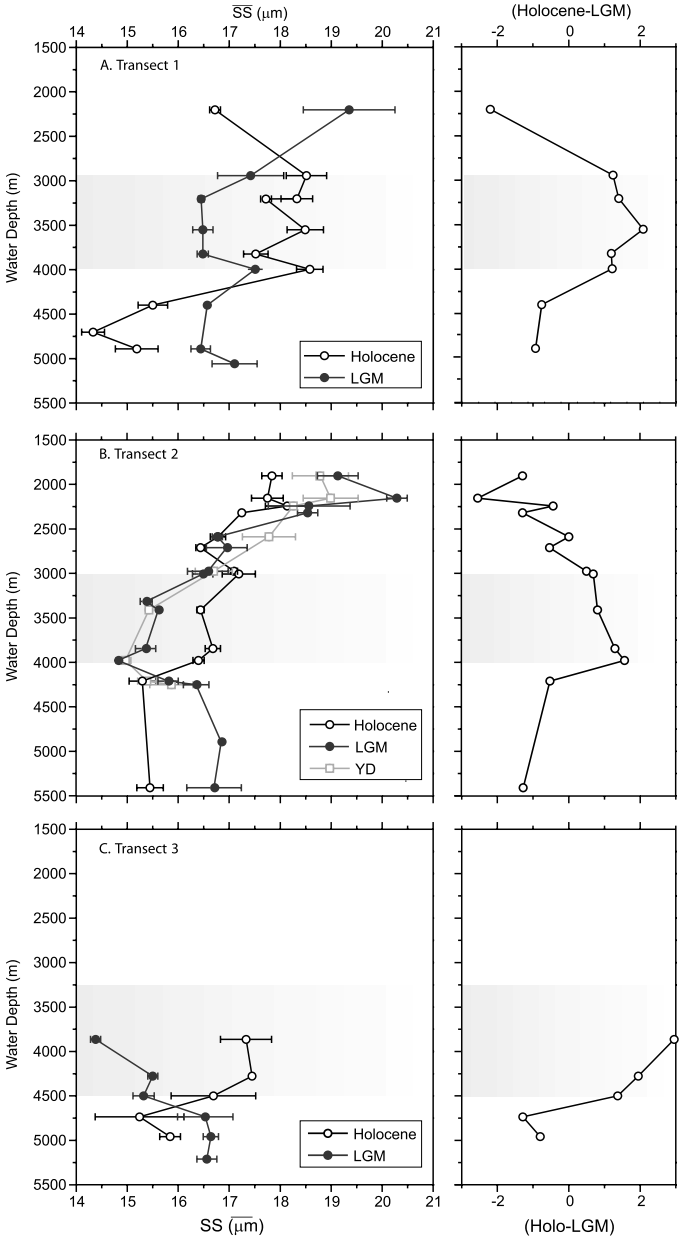

Figure 4. The left side shows the sortable silt mean ($\overline{SS}$) measured on Holocene (black), LGM (light grey) and YD (dark grey) samples where available. Each point represents an average value of 3–5 $\overline{SS}$ measurements with bars showing the 1σ standard deviation at each depth. The right side shows the deviation between the Holocene and LGM samples. (a) Averaged $\overline{SS}$ measurements along transect 1 seaward of the BOR, (b) averaged $\overline{SS}$ measurements along transect 2 down the crest of the BOR, and (c) averaged $\overline{SS}$ measurements along transect 3 down the eastern flank of the BOR. It should be noted that YD measurements are only available on a selection of cores from transect 2, where age constraints and sedimentation rates are most favorable [*Keigwin*, 2004; *Keigwin and Schlegel*, 2002]. The shaded panels represent the depth range influenced by the modern fast flowing core of the WBUC according to the hydrographic measurements of *Stahr and Sanford* [1999].

dance peaks during the YD [*Keigwin*, 2004]. However, the cores used in this study had been already heavily sampled around the YD enabling only small samples to be collected, reducing the numbers of benthic foraminifera available for analysis. The few available samples, however, show a pattern of benthic $\delta^{13}C$ values similar to that previously described for the LGM, with values of >1‰ above 2500 m water depth consistent with a well ventilated, nutrient depleted, NSW mass.

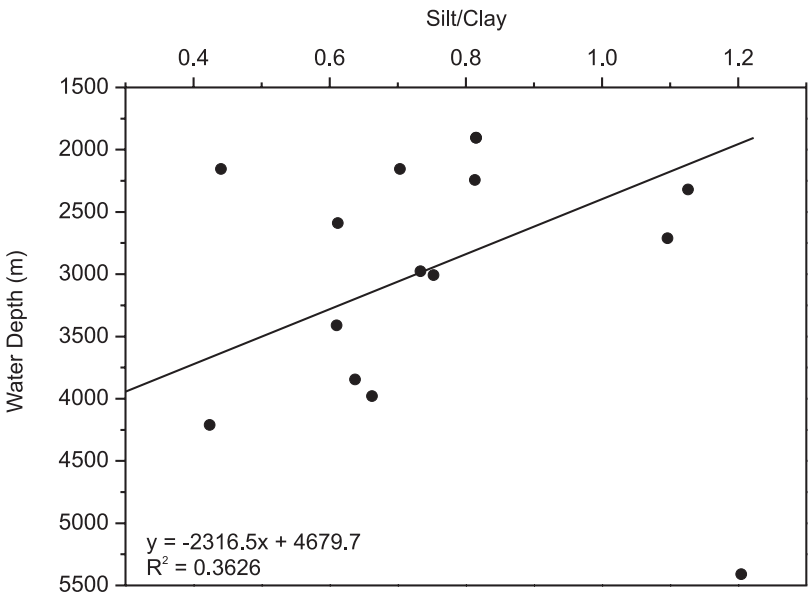

Figure 5. The relationship between the silt/clay ratio of the sediment with depth along the crest of the ridge during the Holocene. Each point represents an average of 3–5 measurements.

Below 2500 m water depth benthic $\delta^{13}C$ values decrease with depth to lighter values more representative of SSW.

5. Discussion

5.1. Holocene

[25] Previous studies on the BOR [*Haskell and Johnson*, 1993], have suggested that Holocene sediment texture and composition were only influenced by the intensity and shifts of the WBUC's zone of maximum flow speed on the flanks of the ridge, while the sediment texture on the crest of the ridge was dominated by fining in the grain size with proximity to the continental margin and the sediment source areas. *Haskell and Johnson* [1993] found no direct indication of the WBUC influence on the ridge crest even where the major axis of the WBUC crossed the crest above 4200 m water depth. This differs markedly to the results presented here in which all three transects show a coarsening of the $\overline{SS}$ between ~3000–4000 m water depth in T1 and T2 and above 4500 m water depth in T3, consistent with the influence of the fast flowing core of the WBUC (15–30 cm s^{-1}) from modern hydrographic sections [*Stahr and Sanford*, 1999]. If these sediment cores were only affected by proximity to the continental margin such increases in $\overline{SS}$ would not occur. Furthermore, the hydrographic survey of *Johns et al.* [1997] in 1990, using a reference section at 26.5°N, reported 20 Sv of the WBUC crossing the crest of the BOR and only 11 Sv flowing around its tip and therefore it is unsurprising that the WBUC fast flowing core influences the grain size records along the crest of the ridge as well as on the flanks. While we cannot rule out that proximity to the continental margin has some influence on the $\overline{SS}$ grain size distribution along the crest of the ridge, our data certainly suggest it is not the dominant influence. The difference between our results and *Haskell and Johnson* [1993] is most likely the result of the different grain size fractions used in the two studies. The 6–70 μm fraction used by *Haskell and Johnson* [1993] includes part of the fine cohesive silt fraction, which tends not to be size-sorted by the current, but rather is deposited as aggregates [*McCave et al.*, 1995; *McCave and Hall*, 2006]. In comparison, the $\overline{SS}$ fraction varies independently of sediment supply in areas of current-sorted muds, allowing it to become an established proxy for flow speed in many locations (see review by *McCave and Hall* [2006]). The fining in the mean grain size record of *Haskell and Johnson* [1993] along the crest of the ridge is likely to result from an increased abundance of fine fraction which is not current sorted. This is consistent with the silt/clay ratios we observe showing increasing clay and decreasing silt content with depth along the crest of ridge (Figure 5), while the $\overline{SS}$ fraction varies independently of depth (Figure 4). This supports the utility of the $\overline{SS}$ fraction in order to study changes in the near bottom flow in

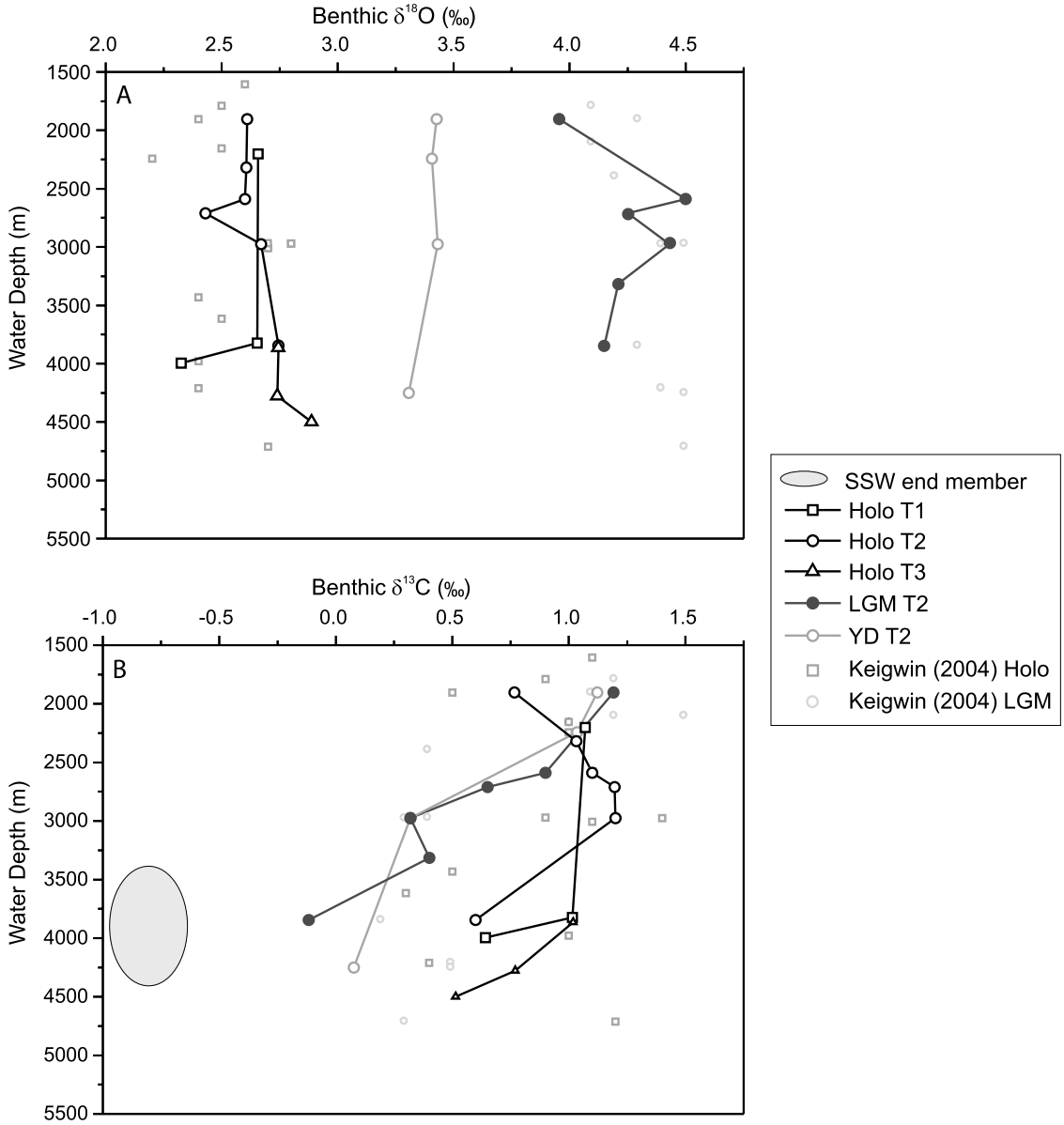

Figure 6. Summary of benthic (a) δ^{13}C and (b) δ^{18}O data from the Holocene (black), the LGM (dark grey), and YD (light grey) time slices. Measurements were made on *Cibicidoides* spp. Squares represent the data from transect 1, circles represent the data from transect 2, and triangles represent the data from transect 3. Solid dark and light grey circles show previous benthic stable isotope measurements from the area during the Holocene and LGM, respectively [*Keigwin*, 2004].

which the influence of smaller cohesive size fractions that are not current sorted are removed [*McCave et al.*, 1995; *McCave and Hall*, 2006].

[26] The Holocene $\overline{SS}$ grain size reconstruction suggests a similar physical hydrography to that based on the measurements of *Stahr and Sanford* [1999] (see shaded panels on Figure 4). *Stahr and Sanford* [1999] record a high velocity core of the WBUC that flows along the bathymetric contours deepening from ~3500 m at its upstream origin to 4100 m further downstream along the eastern flank of the ridge which is consistent with the increase in current intensity between ~3000 m and 4000 m water depth in T1 and along the crest of the ridge, extending as deep as ~4500 m in T3 on the eastern flank of the ridge. Previous reconstructions at the BOR at Sites 1060 (3481 m water depth) and 1062 (4763 m water depth) during the time interval 130–110 ka B.P. (MIS 5d–5e) have also suggested a deepening of the WBUC fast flowing core to ~4000 m water depth during the last interglacial

(MIS 5e [*Bianchi et al.*, 2001]). However, the coarser $\overline{SS}$ values at T1 compared to T2 (difference of ~2 μm) are suggestive of a relative slowing of the fast flowing WBUC core between these two transects. A possible explanation for this is that T1 is located close to where the southward flowing WBUC first intercepts the BOR and is topographically steered toward the southeast. As the current is steered it also accelerates producing the higher $\overline{SS}$ values at T1, in agreement with previous observations of *Stahr and Sanford* [1999] showing higher velocities further up-slope at the BOR. As the ridge slopes progressively deeper toward the abyssal plain, water is transported across the ridge crest. This water is no longer steered and constrained by the topography and may therefore slow down. T2 also reveals fast flow speeds at depths shallower than 2500 m which are likely to reflect the influence of the secondary fast flowing core of the WBUC along the crest of the ridge which is mainly composed of (S)LSW at these depths today [*Johns et al.*, 1997]. Its influence extends from 1000 m to 2500 m water depth, consistent with the $\overline{SS}$ data presented in this study, and reaches current speeds of ~15 cm s^{-1} [*Stahr and Sanford*, 1999].

[27] Below 4200 m water depth at T1 and T2 and 4500 m water depth at T3 flow speeds are lower during the Holocene (Figure 4), suggesting little current activity at these abyssal depths, consistent with the physical hydrographic measurements [*Stahr and Sanford*, 1999]. *Haskell and Johnson* [1993] observed a small increase in mean grain size values at ~5000 m water depth in their ridge crest reconstruction and attributed it to either the presence of a vigorous deeper circulation system or the influence of a distal turbidity current from the Hatteras Abyssal Plain. We find no evidence for a deeper circulation system during the Holocene and the hydrographic measurements of *Stahr and Sanford* [1999] show no evidence in support of a vigorous deeper circulation during the Holocene. Furthermore, previous grain size reconstructions at the BOR have suggested that the WBUC fast flowing core did not influence the depth of Site 1062 (4763 m water depth) during previous warm interglacial/interstadial intervals [*Bianchi et al.*, 2001; *Yokokawa and Franz*, 2002]. We suggest that the core-top increase in grain size recorded by *Haskell and Johnson* [1993] is therefore likely to be the result of a recent event which is not recorded in our averaged Holocene records.

[28] Overall, this suggests that the $\overline{SS}$ grain size proxy can provide a reliable reconstruction of averaged spatial flow speed variability at the BOR during the Holocene that appear consistent with modern hydrographic observations. This allows increased confidence when using the $\overline{SS}$ proxy to interpret relative flow speed changes throughout the last glacial cycle in this region.

[29] The Holocene bathymetric profiles of benthic $\delta^{13}C$ are consistent with the modern configuration of water masses intersecting the BOR and correlate well with the GEOSECS $\delta^{13}C$ profile from the western North Atlantic [*Kroopnick*, 1985; *Curry and Oppo*, 2005] and are also consistent with the Holocene western Atlantic Cd/Ca transect [*Marchitto and Broecker*, 2006]. The benthic $\delta^{13}C$ maximum associated with nutrient-depleted NADW (~1‰) dominates the region above 4000 m water depth, consistent with the modern position of NADW and the fast flowing zone of the WBUC shown in hydrographic profiles [*Amos et al.*, 1971; *Hogg*, 1983; *Stahr and Sanford*, 1999]. The slightly lower benthic $\delta^{13}C$ (0.75–0.5‰) found at depths below 4000 m are consistent with the increased influence of nutrient-enriched, corrosive SSW [*Hogg*, 1983].

5.2. LGM

[30] During the LGM (23–18 ka B.P.) surface waters in the North Atlantic were less dense than their modern day analogue, which resulted in a reduced rate of formation and/or depth penetration of NADW [e.g., *Broecker et al.*, 1985; *Lynch-Steiglitz et al.*, 2007]. Furthermore, ocean models suggest there not only existed a shallower mode of deepwater production during the LGM, but there was also a southward shift in production away from the Nordic Seas to ~50°–60°N [*Rahmstorf*, 1994, 2002; *Ganopolski et al.*, 1998]. However, decreased production in the North may have been balanced by increased production of SSW [e.g., *Crowley*, 1992; *Broecker*, 1998; *Hall et al.*, 2001]. The vertical shift in the zone of maximum flow speed of the WBUC documented by previous studies on the BOR [e.g., *Johnson et al.*, 1988; *Haskell et al.*, 1991; *Bianchi et al.*, 2001; *Yokokawa and Franz*, 2002; *Hall and Becker*, 2007] has been suggested to be linked to the changes in production of NSW described above.

[31] All 3 transects in this study show that a markedly different circulation pattern was present during the LGM compared with Holocene, with the relative slow flow speeds between 3000–4000 m water depth implying that the fast flowing core of the WBUC had shifted and/or weakened. Although

the $\overline{SS}$ proxy is at present uncalibrated, *Ledbetter* [1986] proposed a calibration between the mean grain size of the total terrigenous silt fraction and flow speed. If the LGM and Holocene $\overline{SS}$ difference of ~2 μm at 3000–4000 m water depth is compared to this calibration then a change of ~5 cm s^{-1} is implied. The increase in relative flow speeds above ~2500 m to values higher than those associated with the Holocene in both T1 and T2 suggests that the WBUC fast flowing core had most likely shifted relative to its Holocene depth to a more intermediate depth. This is consistent with previous grain size work on the BOR, which suggests that prior to 12 ka and post LGM, circulation was focused on the upper part of the ridge above 2700 m [*Haskell et al.*, 1991], while during the glacial intervals within MIS 10–8 the WBUC's zone of maximum flow speeds shifted to around ~2200 m [*Yokokawa and Franz*, 2002].

[32] The shift of the WBUC's zone of maximum flow speed to shallower depths is consistent with the benthic $\delta^{13}C$ records presented here and in previous studies, indicating a decrease in the influence of LNADW during the LGM and its replacement with shallower, nutrient-depleted GNAIW [e.g., *Boyle and Keigwin*, 1987; *Oppo and Fairbanks*, 1987; *Curry et al.*, 1988; *Duplessy et al.*, 1988; *Oppo and Lehman*, 1993; *Slowey and Curry*, 1995; *Marchitto et al.*, 1998; *Keigwin and Schlegel*, 2002; *Keigwin*, 2004; *Curry and Oppo*, 2005; *Marchitto and Broecker*, 2006]. *Marchitto et al.* [1998] suggest that an inverse relationship exists between the formation of these deep and intermediate water masses (when LNADW production is strong, GNAIW is absent and vice versa) both on orbital and millennial timescales. Previous shifts of the WBUC's zone of maximum flow speed to shallower depths documented during MIS 5e and 5d (130–110 ka B.P.) at the BOR have been related to reductions in LNADW formation [e.g., *Bianchi et al.*, 2001]. A similar interpretation may explain the shift in the zone of maximum flow speed to shallower depths revealed by the $\overline{SS}$ records during the LGM in conjunction with the development of vigorous but shallow GNAIW. The reconstructed benthic $\delta^{13}C$ profiles for the BOR region, show that this vigorous intermediate depth circulation is indeed associated with the presence of nutrient depleted NSW, consistent with GNAIW (end-member value of 1.5‰ [*Curry and Oppo*, 2005]), with a significant increase in the depth range influenced by SSW (end-member value of −0.2‰ [*Curry and Oppo*, 2005]) below. *Oppo and Lehman* [1993] and *Bertram et al.* [1995] suggest that the transition between GNAIW and SSW was very abrupt in the subpolar North Atlantic with a 1‰ decrease in $\delta^{13}C$ across a 500 m depth interval, centered on ~2000 m. However, *Keigwin* [2004] found that this is not the case in the subtropical western North Atlantic as the benthic $\delta^{13}C$ decreases continuously with depth suggesting a large mixing zone between GNAIW and SSW, a feature in agreement with this study (Figure 6b). However, the deep benthic $\delta^{13}C$ values in the subtropical North Atlantic are heavier than records from the deep South Atlantic [*Curry and Oppo*, 2005], suggesting that waters originating in the North Atlantic also contributed via mixing to the water mass below 2500 m.

[33] The volume flux of glacial NSW water remains equivocal, with some suggesting vigorous renewal of GNAIW [*Gherardi et al.*, 2005; *Hall et al.*, 2006], with a reduction in deepwater export from the North Atlantic of 30–50% during the LGM [*LeGrand and Wunsch*, 1995; *Seidov et al.*, 1996; *Marchal et al.*, 2000; *McManus et al.*, 2004], while other, predominantly modeling, studies hint at similar (or possibly stronger) NSW flow rates to the present-day [e.g., *Yu et al.*, 1996; *Kitoh et al.*, 2001; *Hewitt et al.*, 2003]. While local flow speeds during the LGM are high at shallow depths on the BOR, consistent with enhanced intermediate water production, this is not the only mechanism by which the elevated flow speeds could be produced at the BOR. Alternatively, local changes in the density structure of the WBUC at the LGM may have led to the development of a high velocity jet in the lower part of the nutrient-depleted GNAIW. *Lynch-Stieglitz et al.* [1999] used benthic foraminiferal $\delta^{18}O$ as a proxy for seawater density, as both the $\delta^{18}O$ of calcite and the density of seawater increase as a result of increasing salinity or decreasing temperature. Consideration of the LGM T2 and *Keigwin* [2004] benthic $\delta^{18}O$ data shown in Figure 6a might suggest the presence of a pycnocline between ~2400–2600 m water depth. If this were the case then the enhanced density gradient may have provided the locus for the development of a fast flowing jet along the BOR. However, clearly, variability in the deeper LGM T2 profile suggests that benthic $\delta^{18}O$ may not be linked to density in a straight forward way.

[34] The higher flow speeds below 4000 m water depth during the LGM compared with the Holocene (most obvious in T2) suggests the possibility of a vigorously flowing abyssal circulation at this time. Even though few cores were available for

analysis below 4000 m water depth with both their LGM and Holocene sediments preserved, the higher $\overline{SS}$ values during the LGM are a consistent feature of all cores sampled. This suggests that the increase in flow speeds at depths greater than 4000 m is a robust feature of the WBUC system at the BOR. The benthic $\delta^{13}C$ signature suggest that the water mass feeding this vigorous circulation is of a southern origin, with a benthic $\delta^{13}C$ of >0.5‰ below 4000 m water depth. Furthermore, *Robinson et al.* [2005] found that the pattern of deep sea $\Delta^{14}C$ during the LGM varied synchronously with the atmosphere and suggested that this could result from either vigorous SSW circulation [*Reimer et al.*, 2004] or the occurrence of extensive sea-ice coverage in the Southern Ocean which reduced the air-sea carbon exchange. Combined with our $\overline{SS}$ results we suggest that the results of *Robinson et al.* [2005] are consistent with vigorous SSW flow during the LGM.

[35] It is well documented that a large range in factors (e.g., air-sea exchange, carbonate saturation state, oxidation of organic matter in sediments) can contribute to the $\delta^{13}C$ of benthic foraminiferal shells and potentially decouple $\delta^{13}C$ regionally from global nutrient stoichiometry [e.g., *Broecker and Maier-Reimer*, 1992; *Zahn and Keir*, 1994; *Lynch-Stieglitz*, 2003]. However, the complementary nature of the hydrographic and dynamical reconstructions using the $\overline{SS}$ and benthic $\delta^{13}C$ proxies shown in this study gives increased confidence in their combined use as circulation tracers in this region.

5.3. Younger Dryas

[36] The Younger Dryas is characterized by a return to near glacial temperatures in most of the Northern Hemisphere [*Grootes and Stuiver*, 1997] between 13–11.5 ka B.P. At present the detailed role of changes in the MOC and the WBUC during the YD remains poorly constrained [*McManus et al.*, 2004]. Some early studies suggest that Late Holocene-style deepwater production was established before and during most of the YD [*Sarnthein et al.*, 1994], but most paleodata consistently show that this was not the case [e.g., *Marchitto et al.*, 1998; *Zahn and Stüber*, 2002; *McManus et al.*, 2004], with recent evidence based on $\Delta^{14}C$ ventilation ages [*Keigwin and Schlegel*, 2002; *Keigwin*, 2004] suggesting the replacement of NADW by GNAIW with nutrient rich SSW at depth, similar to LGM, and the stadial circulation mode of *Rahmstorf* [2002].

[37] The combined $\overline{SS}$, and benthic $\delta^{13}C$ data presented in this study strongly suggest that both the physical and chemical hydrography in the western subtropical North Atlantic were similar at the time of the YD and the LGM, with a shallower zone, above 2,500 m water depth, of maximum flow speeds within the WBUC consistent with nutrient depleted GNAIW formation [*Boyle and Keigwin*, 1987; *Oppo and Lehman*, 1993]. This supports previous observations from the BOR made from $\Delta^{14}C$ ventilation ages [*Keigwin*, 2004]. The results of *Keigwin* [2004] revealed similar ventilation ages of ~1000 years below 2300 m during both the LGM and YD consistent with the modeling results of *Stocker and Wright* [1998] indicating an increasing influence of SSW. Although no LGM benthic and planktonic foraminifera pairs were available for ^{14}C AMS dating above 2300 m water depth, YD pairs reveal ventilation ages similar to the present-day (<500 years) consistent with the production of well ventilated GNAIW. This is supported by both the $\overline{SS}$ and benthic $\delta^{13}C$ data which shows that there was vigorous, well ventilated circulation above 2500 m on the BOR during the YD similar to that previously described for the LGM reconstruction. Previous grain size studies at the BOR have hinted at an increased vigor of a shallow circulation above 2700 m water depth during the YD [e.g., *Haskell et al.*, 1991], which is consistent with nutrient depleted GNAIW formation [*Boyle and Keigwin*, 1987; *Marchitto et al.*, 1998]. The data also hint at an increase in SSW vigor at depths below 4000 m during the YD although there are too few records below this depth to draw any firm conclusions.

6. Conclusions

[38] This study demonstrates that changes in $\overline{SS}$ can be used successfully as a proxy to reconstruct changes in deepwater circulation patterns and provides the capability of recording in detail shifts in both the position and strength of the maximum flow axis of the WBUC when compiled as a depth transect. Contrary to the grain size results of previous studies which used the 6–70 μm sediment fraction, the $\overline{SS}$ results in this study suggest that the effects of the fast flowing core of the WBUC on sediments can be observed along the crest of the BOR between ~3000–4000 m water depth. This is consistent with previous hydrographic studies in the area [*Stahr and Sanford*, 1999]. The LGM reconstruction suggests a very different hydrographic pattern was present during this interval

compared with the Holocene, with a shift in the axis of maximum flow speed of WBUC from its Holocene position (3000–4000 m water depth) to <2500 m water depth. Such a change is consistent with a reduced influence of LNADW and increased production of GNAIW. This is in agreement with both previously published [e.g., *Keigwin*, 2004; *Curry and Oppo*, 2005] and our additional benthic $\delta^{13}C$ data from the region. Although the influence of local changes in the density structure of the WBUC at the BOR could also plausibly explain the development of the shallower fast flowing waters. The deep cores selected for this study further suggest an increase in flow speed below 4000 m water depth hinting at an increase in SSW flow speeds during the LGM. Furthermore, both the $\overline{SS}$ and benthic $\delta^{13}C$ records suggest that a similar pattern of circulation was present during the YD as during the LGM. It also appears that cores on the crest of the ridge provide the greatest potential for further grain size work due to their high sedimentation rates and good preservation providing the largest numbers of foraminifera suitable for coupled stable isotope investigations. We support the use of more than one core when studying time series records in order to track the vertical movement of the high velocity core of the WBUC. The position of the axis of maximum WBUC flow reconstructed in this study during the extremes of the Holocene and LGM should aid the interpretation of further downcore time series records.

Acknowledgments

[39] We are grateful to H. Medley for laboratory assistance and G. Bianchi, L. Keigwin, and I. N. McCave for useful discussions. We would also like to thank the core repositories at WHOI and LDEO for assistance and use of facilities when sampling the cores used in this study. L. Carter and L. Skinner are also thanked for their helpful comments. This work was supported by funding from the U. K. National Environmental Research Council (NERC).

References

Alley, R. B., et al. (1993), Abrupt increase in snow accumulation at the end of the Younger Dryas event, *Nature*, *362*, 527–529.

Amos, A. F., A. L. Gordon, and E. D. Schneider (1971), Water masses and circulation patterns in the region of the Blake-Bahama Outer Ridge, *Deep Sea Res. Oceanogr. Abstr.*, *18*, 145–165.

Barranco, F. T., Jr., W. L. Balsam, and B. C. Deaton (1989), Quantitative reassessment of brick red lutites: Evidence from reflective spectrophotometry, *Mar. Geol.*, *89*, 299–314.

Bertram, C. J., H. Elderfield, N. J. Shackleton, and J. A. Macdonald (1995), Cadmium/calcium and carbon-isotope reconstructions of the glacial northeast Atlantic-Ocean, *Paleoceanography*, *10*, 563–578.

Bianchi, G. G., I. R. Hall, I. N. McCave, and L. Joseph (1999), Measurement of the sortable silt current speed proxy using the Sedigraph 5100 and Coulter Multisizer IIe: Precision and accuracy, *Sedimentology*, *46*, 1001–1014.

Bianchi, G. G., M. Vautravers, and N. J. Shackleton (2001), Deep flow variability under apparently stable North Atlantic Deep Water production during the last interglacial of the subtropical NW Atlantic, *Paleoceanography*, *16*, 306–316.

Boyle, E. A., and L. D. Keigwin (1987), North Atlantic thermohaline circulation during the past 20,000 years linked to high-latitude surface temperature, *Nature*, *330*, 35–40.

Broecker, W. S. (1998), Paleocean circulation during the last deglaciation: A bipolar seesaw?, *Paleoceanography*, *13*(2), 119–121.

Broecker, W. S., and E. Maier-Reimer (1992), The influence of air and sea exchange on the carbon isotope distribution in the sea, *Global Biogeochem. Cycles*, *6*(3), 315–320.

Broecker, W. S., D. M. Peteet, and D. Rind (1985), Does the ocean-atmosphere system have more than one stable mode of operation?, *Nature*, *315*, 21–26.

Bryan, G. M. (1970), Hydrodynamic model of the Blake Outer Ridge, *J. Geophys. Res.*, *75*, 4530–4537.

Bulfinch, D. L., and M. T. Ledbetter (1983/1984), Deep Western Boundary Undercurrent delineated by sediment texture at base of North American continental rise, *Geo Mar. Lett.*, *3*, 31–36.

Bulfinch, D. L., M. T. Ledbetter, B. B. Ellwood, and W. L. Balsam (1982), The high-velocity core of the Western Boundary Undercurrent at the base of the U.S. continental rise, *Science*, *215*, 970–973.

Came, R. E., D. W. Oppo, and W. B. Curry (2003), Atlantic Ocean circulation during the Younger Dryas: Insights from a new Cd/Ca record from the western subtropical South Atlantic, *Paleoceanography*, *18*(4), 1086, doi:10.1029/2003PA000888.

Crowley, T. J. (1992), North Atlantic deep water cools the southern hemisphere, *Paleoceanography*, *7*(4), 489–497.

Curry, W. B., and D. W. Oppo (2005), Glacial water mass geometry and the distribution of $\delta^{13}C$ of ΣCO_2 in the western Atlantic Ocean, *Paleoceanography*, *20*, PA1017, doi:10.1029/2004PA001021.

Curry, W. B., J.-C. Duplessy, L. D. Labeyrie, and N. J. Shackleton (1988), Changes in the distribution of $\delta^{13}C$ of deep water ΣCO_2 between the last glaciation and the Holocene, *Paleoceanography*, *3*, 317–341.

Duplessy, J.-C., N. J. Shackleton, R. G. Fairbanks, L. Labeyrie, D. Oppo, and N. Kallel (1988), Deep-water source variations during the last climatic cycle and their impact on the global deep-water circulation, *Paleoceanography*, *3*, 343–360.

Ewing, J., M. Ewing, and R. Leyden (1966), Seismic profile survey of the Blake Plateau, *Am. Assoc. Petrol. Geol. Bull.*, *50*, 1948–1971.

Ganopolski, A., S. Rahmstorf, V. Petoukhov, and M. Claussen (1998), Simulation of modern and glacial climates with a coupled global model of intermediate complexity, *Nature*, *391*(6665), 351–356.

Gherardi, J. M., L. Labeyrie, J. F. McManus, R. Francois, L. C. Skinner, and E. Cortijo (2005), Evidence from the northeastern Atlantic basin for variability in the rate of the meridional overturning circulation through the last deglaciation, *Earth Planet. Sci. Lett.*, *240*, 710–723.

Grootes, P. M., and M. Stuiver (1997), Oxygen 18/16 variability in Greenland snow and ice with 10(−3)- to 10(5)-year time resolution, *J. Geophys. Res.*, *102*(C12), 26,455–26,470.

Hall, I. R., and J. Becker (2007), Deep Western Boundary Current variability in the subtropical northwest Atlantic Ocean during marine isotope stages 12–10, *Geochem. Geophys. Geosyst.*, *8*, Q06013, doi:10.1029/2006GC001518.

Hall, I. R., I. N. McCave, N. J. Shackleton, G. P. Weedon, and S. E. Harris (2001), Intensified deep Pacific inflow and ventilation in Pleistocene glacial times, *Nature*, *412*, 809–812.

Hall, I. R., S. B. Moran, R. Zahn, P. C. Knutz, C.-C. Shen, and R. L. Edwards (2006), Accelerated drawdown of meridional overturning in the late-glacial Atlantic triggered by transient pre-H event freshwater perturbation, *Geophys. Res. Lett.*, *33*, L16616, doi:10.1029/2006GL026239.

Haskell, B. J., and T. C. Johnson (1993), Surface sediment response to deepwater circulation on the Blake Outer Ridge, western North Atlantic: Paleoceanographic implications, *Sediment. Geol.*, *82*, 133–144.

Haskell, B. J., T. C. Johnson, and W. J. Showers (1991), Fluctuations in deep western North Atlantic circulation on the Blake Outer Ridge during the last deglaciation, *Paleoceanography*, *6*, 21–31.

Heezen, B. C., C. D. Hollister, and W. F. Ruddiman (1966), Shaping of the continental rise by deep geostrophic contour currents, *Science*, *152*, 502–508.

Hewitt, C. D., R. J. Stouffer, A. J. Broccoli, J. F. B. Mitchell, and P. J. Valdes (2003), The effect of ocean dynamics in a coupled GCM simulation of the Last Glacial Maximum, *Clim. Dyn.*, *20*, 203–218.

Hogg, N. G. (1983), A note on the deep circulation of the western North Atlantic: Its nature and causes, *Deep Sea Res., Part A*, *9*, 945–961.

Hollister, C. D., and B. C. Heezen (1972), Geologic effects of ocean bottom currents, in *Studies in Physical Oceanography—A Tribute to George Wust on his 80th Birthday*, vol. 2, edited by A. L. Gordon, pp. 37–66, Gordon and Breach, New York.

Hoogakker, B. A. A., I. N. McCave, and M. J. Vautravers (2007), Antarctic link to deep flow speed variation during marine isotope stage 3 in the western North Atlantic, *Earth Planet. Sci. Lett*, *257*(3–4), 463–473.

Johns, E., R. A. Fine, and R. L. Molinari (1997), Deep flow along the western boundary of the Blake Bahama Outer Ridge, *J. Phys. Oceanogr.*, *27*, 2187–2208.

Johnson, T. C., E. L. Lynch, W. J. Showers, and N. C. Placzuk (1988), Pleistocene fluctuations in the Western Boundary Undercurrent on the Blake Outer Ridge, *Paleoceanography*, *3*, 191–207.

Keigwin, L. D. (1996), The Little Ice Age and Medieval Warm Period in the Sargasso Sea, *Science*, *274*, 1504–1508.

Keigwin, L. D. (2004), Radiocarbon and stable isotope constraints on Last Glacial Maximum and Younger Dryas ventilation in the western North Atlantic, *Paleoceanography*, *19*, PA4012, doi:10.1029/2004PA001029.

Keigwin, L. D., and M. A. Schlegel (2002), Ocean ventilation and sedimentation since the glacial maximum at 3 km in the western North Atlantic, *Geochem. Geophys. Geosyst.*, *3*(6), 1034, doi:10.1029/2001GC000283.

Keigwin, L. D., G. A. Jones, and P. N. Froelich (1992), A 15,000 year paleoenvironmental record from Meiji Seamount, far northwestern Pacific, *Earth Planet. Sci. Lett.*, *111*, 425–440.

Keigwin, L. D., et al. (1998), *Proceedings of the Ocean Drilling Program, Initial Reports*, vol. 172, Ocean Drill. Program, College Station, Tex.

Kitoh, A., S. Murakami, and H. Koide (2001), A simulation of the last glacial maximum with a coupled atmosphere-ocean GCM, *Geophys. Res. Lett.*, *28*(11), 2221–2224.

Kroopnick, P. M. (1985), The distribution of C-13 of sigma-CO_2 in the world oceans, *Deep Sea Res., Part A*, *32*(1), 57–84.

Laine, E. P., W. D. Gardner, M. J. Richardson, and M. A. Kominz (1994), Abyssal currents and advection of resuspended sediment along the north-eastern Bermuda Rise, *Mar. Geol.*, *119*, 159–171.

Lea, D. W., and E. A. Boyle (1990), A 210,000-year record of barium variability in the deep northwest Atlantic Ocean, *Nature*, *347*, 269–272.

Leaman, K. D., and P. S. Vertes (1996), Topographic influences on recirculation in the Deep Western Boundary Current: Results from RAFOS float trajectories between the Blake-Bahama Outer Ridge and the San Salvador 'Gate', *J. Phys. Oceanogr.*, *26*, 941–961.

Ledbetter, M. T. (1986), Bottom-current pathways in the Argentine Basin revealed by mean silt particle size, *Nature*, *321*, 423–425.

Ledbetter, M. T., and W. L. Balsam (1985), Paleoceanography of the Deep Western Boundary Undercurrent on the North American continental margin for the past 25000 yr, *Geology*, *13*, 181–184.

Lee, T. N., W. E. Johns, R. J. Zantopp, and E. R. Fillenbaum (1996), Moored observations of western boundary current variability and thermocline circulation at 26.5′N in the subtropical North Atlantic, *J. Phys. Oceanogr.*, *26*, 962–983.

LeGrand, P., and C. Wunsch (1995), Constraints from paleotracer data on the North Atlantic circulation during the last glacial maximum, *Paleoceanography*, *10*(6), 1011–1045.

Loubere, P. (1991), Deep-sea benthic foraminiferal assemblage response to a surface ocean productivity gradient: A test, *Paleoceanography*, *6*, 193–204.

Loubere, P. (2000), Marine control of biological production in the eastern equatorial Pacific Ocean, *Nature*, *406*, 497–500.

Lynch-Stieglitz, J. (2003), Tracers of past ocean circulation, in *Treatise on Geochemistry*, vol. 6, *The Oceans and Marine Geochemistry*, edited by H. Elderfield, vol. 6, pp. 433–451, Elsevier, New York.

Lynch-Stieglitz, J., W. B. Curry, and N. Slowey (1999), Weaker Gulf Stream in the Florida Straits during the Last Glacial Maximum, *Nature*, *402*, 644–648.

Lynch-Steiglitz, J., et al. (2007), Atlantic meridional overturning circulation during the Last Glacial Maximum, *Science*, *316*(5821), 66–69.

Manabe, S., and R. Stouffer (1997), Coupled ocean-atmosphere model response to freshwater input: Comparison to Younger Dryas event, *Paleoceanography*, *12*, 321–336.

Marchal, O., R. Francois, T. F. Stocker, and F. Joos (2000), Ocean thermohaline circulation and sedimentary $^{231}Pa/^{230}Th$ ratio, *Paleoceanography*, *15*, 625–641.

Marchitto, T. M., and W. S. Broecker (2006), Deep water mass geometry in the glacial Atlantic Ocean: A review of constraints from the paleonutrient proxy Cd/Ca, *Geochem. Geophys. Geosyst.*, *7*, Q12003, doi:10.1029/2006GC001323.

Marchitto, T. M., W. B. Curry, and D. W. Oppo (1998), Millennial-scale changes in North Atlantic circulation since the last glaciation, *Nature*, *393*(6685), 557–561.

McCartney, M. S. (1993), Crossing of the equator by the deep western boundary current in the Western Atlantic Ocean, *J. Phys. Oceanogr.*, *23*, 1953–1974.

McCave, I. N., and I. R. Hall (2006), Size sorting in marine muds: Processes, pitfalls, and prospects for paleoflow-speed proxies, *Geochem. Geophys. Geosyst.*, *7*, Q10N05, doi:10.1029/2006GC001284.

McCave, I. N., B. Manighetti, and S. G. Robinson (1995), Sortable silt and fine sediment size/composition slicing:

Parameters for palaeocurrent speed and palaeoceanography, *Paleoceanography*, *10*, 593–610.

McManus, J. F., R. Francois, J.-M. Gherardi, L. D. Keigwin, and S. Brown-Leger (2004), Collapse and rapid resumption of Atlantic meridional circulation linked to deglacial climate changes, *Nature*, *428*, 834–837.

Mix, A. C., and R. G. Fairbanks (1985), North Atlantic surface-ocean control of Pleistocene deep-ocean circulation, *Earth Planet. Sci. Lett.*, *73*, 231–243.

Oppo, D. W., and R. G. Fairbanks (1987), Variability in the deep and intermediate water circulation of the Atlantic Ocean during the past 25,000 years: Northern Hemisphere modulation of the Southern Ocean, *Earth Planet. Sci. Lett.*, *86*, 1–15.

Oppo, D. W., and S. J. Lehman (1993), Mid-depth circulation of the subpolar North Atlantic during the Last Glacial Maximum, *Science*, *259*, 1148–1152.

Orsi, A. H., S. S. Jacobs, A. L. Gordon, and M. Visbeck (2001), Cooling and ventilating the abyssal ocean, *Geophys. Res., Lett.*, *28*, 2923–2926.

Pickart, R. S. (1992), Water mass components of the North-Atlantic Deep Western Boundary Current, *Deep Sea Res., Part A*, *39*(9), 1553–1572.

Rahmstorf, S. (1994), Rapid climate transitions in a coupled ocean-atmosphere model, *Nature*, *372*(6501), 82–85.

Rahmstorf, S. (2002), Ocean circulation and climate during the past 120,000 years, *Nature*, *419*, 207–214.

Reimer, P. J., et al. (2004), IntCal04 terrestrial radiocarbon age calibration, 0–26 cal kyr BP, *Radiocarbon*, *46*(3), 1029–1058.

Richardson, M. J., M. Wimbush, and L. Mayer (1981), Exceptionally strong near-bottom flows on the continental rise of Nova-Scotia, *Science*, *231*(4510), 887–888.

Robinson, L. F., J. F. Adkins, L. D. Keigwin, J. Southon, D. P. Fernandez, S. L. Wang, and D. S. Scheirer (2005), Radiocarbon variability in the western North Atlantic during the last deglaciation, *Science*, *310*(5753), 1469–1473.

Sarnthein, M., K. Winn, S. J. A. Jung, J.-C. Duplessy, L. Labeyrie, H. Erlenkeuser, and G. Ganssen (1994), Changes in east Atlantic deepwater circulation over the last 30,000 years: Eight time slice reconstructions, *Paleoceanography*, *9*(2), 209–267.

Seidov, D., M. Sarnthein, K. Stattegger, R. Prien, and M. Weinelt (1996), North Atlantic ocean circulation during the last glacial maximum and subsequent meltwater event: A numerical model, *J. Geophys. Res.*, *101*(C7), 16,305–16,332.

Shackleton, N. J. (1974), Attainment of isotopic equilibrium between ocean water and benthonic foraminifera genus Uvigerina: Isotopic changes in the ocean during the last glacial, *Cent. Natl. Rech. Sci. Colloq. Int.*, *219*, 203–210.

Slowey, N. C., and W. B. Curry (1995), Glacial-interglacial differences in circulation and carbon cycling within the upper western North Atlantic, *Paleoceanography*, *10*(4), 715–732.

Stahr, F. R., and T. B. Sanford (1999), Transport and bottom boundary layer observations of the North Atlantic Deep Western Boundary Current at the Blake Outer Ridge, *Deep Sea Res., Part II*, *46*, 205–243.

Stocker, T. F., and D. G. Wright (1998), The effect of a succession of ocean ventilation changes on ^{14}C, *Radiocarbon*, *40*, 359–366.

Stuiver, M., P. J. Reimer, and R. W. Reimer (2005), CALIB Radiocarbon Calibration: Execute Version 5.0.2html, operating instructions, Queens University Belfast, Belfast, U. K. (Available at http://radiocarbon.pa.qub.ac.uk/calib/)

Weatherly, G. L., and E. A. Kelley (1984), Two views of the cold filament, *J. Phys. Oceanogr.*, *15*, 68–81.

Yokokawa, M., and S.-O. Franz (2002), Changes in grain size and magnetic fabric at the Blake-Bahama Outer Ridge during the late Pleistocene (marine isotope stages 8–10), *Mar. Geol.*, *189*, 123–144.

Yu, E.-F., R. Francois, and M. P. Bacon (1996), Similar rates of modern and last-glacial ocean thermohaline circulation inferred from radiochemical data, *Nature*, *379*, 689–694.

Zahn, R., and R. Keir (1994), Tracer-nutrient correlations in the upper ocean: Observational and box model constraints on the use of benthic foraminiferal $\delta^{13}C$ and Cd/Ca as paleoproxies for the intermediate-depth ocean, in *Carbon Cycle in the Glacial Ocean: Constraints on the Ocean's Role in Global Change*, *NATO ASI Ser., Ser. 1*, vol. 17, edited by R. Zahn et al., pp. 195–221, Springer, Berlin.

Zahn, R., and A. Stüber (2002), Suborbital intermediate water variability inferred from paired benthic foraminiferal Cd/Ca and $\delta^{13}C$ in the tropical West Atlantic and linking with North Atlantic climates, *Earth Planet. Sci. Lett.*, *200*, 191–205.

Zahn, R., K. Winn, and M. Sarnthein (1986), Benthic foraminiferal $\delta^{13}C$ and accumulation rates of organic carbon: *Uvigerina peregrina* group and *Cibididoides wuellerstorfi*, *Paleoceanography*, *1*, 27–42.